

Hydrogenated Amorphous Silicon (a-Si:H) Colloids

Justin T. Harris, José L. Hueso, and Brian A. Korgel*

Department of Chemical Engineering, Texas Materials Institute, Center for Nano- and Molecular Science and Technology, The University of Texas at Austin, Austin, Texas 78712, United States

Received August 30, 2010. Revised Manuscript Received November 1, 2010

Colloidal particles of hydrogenated amorphous silicon (a-Si:H) were synthesized by decomposition of trisilane (Si_3H_8) in supercritical *n*-hexane (sc-hexane) at temperatures ranging from 380 to 550 °C. The reaction temperature, pressure and Si_3H_8 concentration have a significant influence on the average particle size, Si bond order and hydrogen content. The particle diameter could be varied from 170 nm to 1.7 μm , with hydrogen loadings between 10% and 58%. Raman spectroscopy of the particles revealed significant differences in Si bond order that correlated with hydrogen content, with the lowest reaction temperatures yielding particles with the least structural order and most associated hydrogen. Particles synthesized at temperatures higher than 420 °C had sufficient bond order to allow crystallization under the Raman laser probe.

Introduction

Hydrogenated amorphous silicon (a-Si:H) has a wide variety of uses, including memory switching devices,^{1,2} light-emitting diodes,³ thin film transistors,⁴ and solar cells.⁵ For these applications, layers of a-Si:H are usually vapor-deposited on substrates. However, a variety of other applications would benefit from the availability of large quantities of a-Si:H particles. Fuel cells, for example, require a safe and efficient way to store hydrogen.⁶ Nanoparticles of amorphous Si have high surface area-to-volume ratios and an ability to bond H,⁷ and unlike the effective, yet reactive, solid metal hydrides,⁶ such as MgH_2 and LiBH_4 ,^{8–10} are not dangerous. Hydrogen reversibly bonds to both crystalline and amorphous Si,^{11,12} but a-Si has an advantage over crystalline Si since H can penetrate the amorphous structure and loading is

not limited to surface adsorption. In fact, nanostructured a-Si has been shown to absorb up to 50 atomic % hydrogen, or 3.4% hydrogen by weight.¹³ Another possible application of a-Si nanoparticles is as an anode material in lithium ion batteries. The theoretical capacity for Li storage in Si of 4212 mAh/g is much higher than that of the standard graphitic anode of 372 mAh/g.¹⁴ Lithiation of Si, however, leads to a massive 400% volume expansion that pulverizes the material and destroys the battery. Nanostructured Si can mechanically tolerate this expansion and might offer a solution to this problem.^{15–18} Since Li incorporation leads to amorphization, it may be suitable to use a-Si nanoparticles as the anode material. For these reasons, there is an interest in developing methods for obtaining significant quantities of dispersed a-Si particles with reasonably narrow size distributions.

One way to generate a-Si particles is by an aerosol process.^{19–22} This approach, however, yields little control over particle size and makes it difficult to produce spherical unaggregated particles larger than 100 nm or so in diameter.

*To whom correspondence should be addressed. E-mail: korgel@che.utexas.edu. Phone: +1-512-471-5633. Fax: +1-512-471-7060.

- (1) Lecomber, P. G.; Owen, A. E.; Spear, W. E.; Hajto, J.; Snell, A. J.; Choi, W. K.; Rose, M. J.; Reynolds, S. J. *Non-Cryst. Solids* **1985**, 77–8, 1373–1382.
- (2) Owen, A. E.; Lecomber, P. G.; Spear, W. E.; Hajto, J. *Non-Cryst. Solids* **1983**, 59–6, 1273–1280.
- (3) Kruangam, D.; Toyama, T.; Hattori, Y.; Deguchi, M.; Okamoto, H.; Hamakawa, Y. *J. Non-Cryst. Solids* **1987**, 97–8, 293–296.
- (4) Snell, A. J.; Mackenzie, K. D.; Spear, W. E.; Lecomber, P. G.; Hughes, A. J. *Appl. Phys.* **1981**, 24, 357–362.
- (5) Carlson, D. E.; Wronski, C. R. *Appl. Phys. Lett.* **1976**, 28, 671–673.
- (6) Bley, R. A.; Kauzlarich, S. M. *J. Am. Chem. Soc.* **1996**, 118, 12461–12462.
- (7) Neiner, D.; Kauzlarich, S. M. *Chem. Mater.* **2010**, 22, 487–493.
- (8) Fichtner, M. *Adv. Eng. Mater.* **2005**, 7, 443–455.
- (9) Friedrichs, O.; Aguey-Zinsou, F.; Fernandez, J. R. A.; Sanchez-Lopez, J. C.; Justo, A.; Klassen, T.; Bormann, R.; Fernandez, A. *Acta Mater.* **2006**, 54, 105–110.
- (10) Mauron, P.; Buchter, F.; Friedrichs, O.; Remhof, A.; Biemann, M.; Zwicky, C. N.; Zuttel, A. J. *Phys. Chem. B* **2008**, 112, 906–910.
- (11) Canaria, C. A.; Huang, M.; Cho, Y.; Heinrich, J. L.; Lee, L. I.; Shane, M. J.; Smith, R. C.; Sailor, M. J.; Miskelly, G. M. *Adv. Funct. Mater.* **2002**, 12, 495–500.
- (12) Vandewalle, C. G.; Street, R. A. *Phys. Rev. B* **1995**, 51, 10615–10618.

- (13) Farjas, J.; Das, D.; Fort, J.; Roura, P.; Bertran, E. *Phys. Rev. B* **2002**, 65, 115403.
- (14) Kasavajjula, U.; Wang, C. S.; Appleby, A. J. *J. Power Sources* **2007**, 163, 1003–1039.
- (15) Chan, C. K.; Patel, R. N.; O'Connell, M. J.; Korgel, B. A.; Cui, Y. *ACS Nano* **2010**, 4, 1443–1450.
- (16) Graetz, J.; Ahn, C. C.; Yazami, R.; Fultz, B. *Electrochem. Solid State Lett.* **2003**, 6, A194–A197.
- (17) Li, H.; Huang, X. J.; Chen, L. Q.; Wu, Z. G.; Liang, Y. *Electrochem. Solid State Lett.* **1999**, 2, 547–549.
- (18) Holzapfel, M.; Buqa, H.; Scheifele, W.; Novak, P.; Petrat, F. M. *Chem. Commun.* **2005**, 1566–1568.
- (19) Onischuk, A. A.; Strunin, V. P.; Ushakova, M. A.; Panfilov, V. N. *Khim. Fiz.* **1994**, 13, 129–138.
- (20) Everstei, F. *Philips Res. Rep.* **1971**, 26, 134.
- (21) Odden, J. O.; Egeberg, P. K.; Kjekshus, A. *Sol. Energy Mater. Sol. Cells* **2005**, 86, 165–176.
- (22) Onischuk, A. A.; Strunin, V. P.; Samoilova, R. I.; Nosov, A. V.; Ushakova, M. A.; Panfilov, V. N. *J. Aerosol Sci.* **1997**, 28, 1425–1441.

A few years ago, we demonstrated the synthesis of colloidal a-Si particles by decomposition of trisilane (Si_3H_8) in supercritical *n*-hexane (sc-hexane) at high temperature.^{23,24} By pressurizing the solvent above its critical point, colloidal solution-phase particle synthesis can be carried out at relatively high temperature. The particles are spherical, relatively monodisperse, not aggregated and easily dispersed in organic solvents. Here, we report that the structural Si bond order and hydrogen content of a-Si:H particles can vary significantly and controllably by modifying the synthesis temperature. When the reaction temperature is increased from 380 to 550 °C, the color of the a-Si particles ranges from bright yellow to deep red to dark purple—these color changes relate to the hydrogen content and the structural order within the particles. Particles synthesized under various conditions were characterized in detail by attenuated total reflection Fourier transform infrared (ATR-FTIR) and Raman spectroscopy.

Experimental Details

Reagents. All chemicals were used as received, without further purification. Trisilane (Si_3H_8 ; 100%) was obtained from Voltaix. (**Caution:** trisilane is pyrophoric and must be handled in inert atmosphere!) *N*-hexane (95%, anhydrous) was obtained from Sigma-Aldrich. Trisilane and *n*-hexane were stored in a nitrogen-filled glovebox. Chloroform (with 0.75% ethanol as preservative) was used as received from Fisher Scientific.

a-Si:H Particle Synthesis. a-Si:H particles were prepared by trisilane decomposition in supercritical *n*-hexane using a home-built batch-scale reactor, similar to that described previously.²³ The cylindrical reactor is solid titanium, with an internal volume of 10 mL and sealed with tapered titanium plugs that are tightened by titanium screws. The reactor is heated in a brass block with two resistive heaters coupled to a Variac controller set at 70% power. The reactor temperature is regulated by a thermocouple inside the heating block. The brass block is insulated with fiberglass in a larger aluminum box. The reaction pressure is controlled by varying the amount of solvent and trisilane added to the 10 mL reactor. The pressures reported here were determined from the *n*-hexane phase diagram.²⁵

A typical reaction is carried out by loading the reactor with *n*-hexane and trisilane in a nitrogen-filled glovebox. The reactor is then sealed, removed from the glovebox and inserted into the heating unit. For example, a typical reaction run at 420 °C and 34.5 MPa (5000 psi) is performed by loading in a nitrogen-filled glovebox the 10 mL titanium reactor with 5.8 mL of *n*-hexane and 25 μL of trisilane. In the meantime, the heating block is preheated to 50 °C (outside the glovebox) above the desired reaction temperature (in this case, 470 °C), with an empty reactor in the block to maintain good thermocouple contact. After sealing the reactor, it is removed from the glovebox and placed into the preheated block. The temperature initially drops to about 40 °C below the desired reaction temperature and returns to the targeted temperature after 2.5 min. After a total of 10 min of heating, the reactor is removed from the heating block

and submerged in an ice bath. **Caution:** DO NOT EXCEED the maximum tolerated pressure and temperature of the reactor! The titanium reactors used for these experiments are not reliable above 69.0 MPa (10000 psi) and 600 °C. Furthermore, caution is required when opening the reactor after reactions carried out with higher trisilane concentrations. For example, when more than 300 μL of Si_3H_8 is added, not all of the Si_3H_8 decomposes in a 10 min reaction and the remaining Si_3H_8 will ignite if the reactor is opened in air.

Once the reactor cools to room temperature (usually after about 10 min in the ice bath), the reactor is opened and the product is collected with 5 mL chloroform. The product is centrifuged at 8000 rpm for 5 min to precipitate the particles. The supernatant is discarded. The particles are redispersed in 2 mL chloroform with light sonication and then stored in ambient atmosphere. This procedure routinely yields product with about a 60% conversion of trisilane to a-Si:H particles on a per Si atom basis.

Materials Characterization. SEM images were obtained using a Zeiss Supra 40 VP SEM operated at 5 keV. The particles were suspended in chloroform and deposited by evaporation on Si substrates and imaged. Size distributions were determined by counting 300 particles for each sample imaged from random areas of the substrate.

TEM images were obtained using a Phillips 208 TEM operated at 80 keV for general imaging, or a JEOL 2010F TEM operated at 200 keV. Particles were dispersed in chloroform at 2.5 mg/mL concentration, and 5 μL of the mixture was dropped onto carbon-coated 200 mesh copper TEM grids (Electron Microscopy Sciences).

X-ray diffraction (XRD) was carried out using a Rigaku R-Axis Spider Diffractometer with Image plate detector with $\text{Cu-K}\alpha$ ($\lambda = 1.542 \text{ \AA}$) radiation operated at 40 kV and 40 mA. Measurements were taken on particles suspended on a 0.5 mm nylon loop. Samples were scanned for 10 min while rotating at 10° per minute at 298 K in ambient atmosphere. The resulting radial data was integrated over 10–90° 2θ and plotted. Background scattering from the nylon loop was subtracted from the sample measurement.

Attenuated total reflection Fourier transform infrared (ATR-FTIR) spectra were acquired with a Thermo Mattson Infinity Gold FTIR with an ATR stage made of crystalline ZnSe. The detector was cooled by liquid nitrogen, and spectra taken by averaging 128 scans from 400 to 4000 cm^{-1} at 1 cm^{-1} resolution. The a-Si:H colloids were dropcast onto the ATR stage from chloroform and dried under a nitrogen gas purge. Background scans were performed on the blank ATR stage after purging the chamber with nitrogen to remove all carbon dioxide and water signals and automatically subtracted from the sample spectra.

Simultaneous thermal gravimetric analysis (TGA) and differential scanning calorimetry (DSC) measurements were performed on a Mettler-Toledo TGA/DSC1. 5–10 mL of each sample were loaded in 70 μL alumina crucibles by dropcasting from chloroform and dried in ambient atmosphere. Samples were heated from 25 to 800 °C at 5 °C/min under a nitrogen atmosphere with an 80 mL/min purge. The hydrogen content in the samples was calculated from the maximum weight loss of the sample without accounting for possible solvent loss or oxidation during the measurement.

Raman spectroscopy was conducted on a Renishaw inVia Microscope equipped with a 514.5 nm Argon laser in back-scattering configuration. The instrument was calibrated to the Stokes Raman signal at 521 cm^{-1} for a bulk single crystal of Si with the [110] direction oriented normal to the laser. The beam

- (23) Pell, L. E.; Schricker, A. D.; Mikulec, F. V.; Korgel, B. A. *Langmuir* **2004**, 20, 6546–6548.
- (24) Rabideau, B. D.; Pell, L. E.; Bonnacaze, R. T.; Korgel, B. A. *Langmuir* **2007**, 23, 1270–1274.
- (25) Yaws, C. L. *Handbook of Thermodynamic Properties*; Gulf Publishing Company: Houston, TX, 1996; Vol. 2.

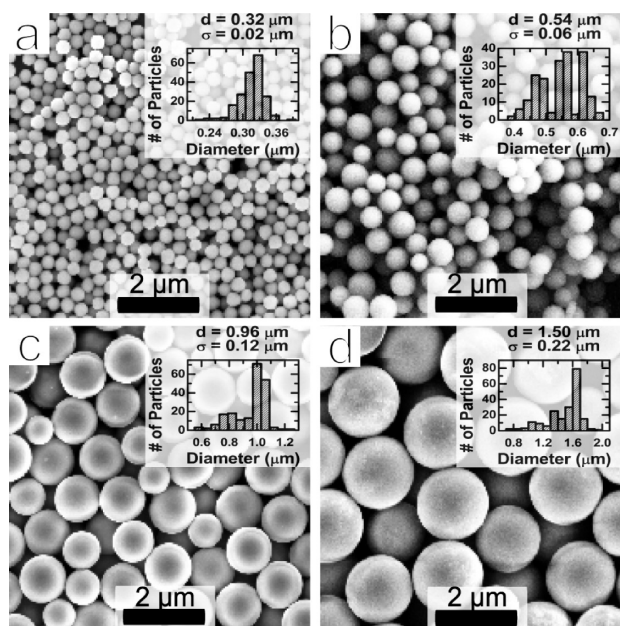


Figure 1. SEM images of a-Si:H particles synthesized in sc-hexane at 420 °C at 34.5 MPa (5000 psi) with different amounts of Si_3H_8 added to the reactor: (a) 20, (b) 60, (c) 100, and (d) 300 μL . Insets: Particles size distributions determined from SEM images.

was focused on the sample using an optical microscope with a 50x objective lens. Samples were prepared by dropcasting the particles from chloroform dispersions onto glass slides. Spectra were obtained by single scans from 100 to 1200 cm^{-1} . The laser power was attenuated during most experiments from 10% (0.35 mW) to 50% (1.5 mW) of the maximum power. Single scans from multiple areas of each sample yielded reproducible Raman spectra. Samples did not exhibit further crystallization after several scans on the same spot at 10% (0.35 mW) laser power. Raman spectra were fitted with Gaussian and Lorentzian–Gaussian curves centered at 470–475 and 490–496 cm^{-1} , respectively,²⁶ to estimate the relative nanocrystalline volume fraction and bond order from the ratios of the integrated areas of the peaks.^{27,28}

Results and Discussion

a-Si:H Particle Synthesis. Figure 1 shows SEM images of a-Si:H particles made by decomposing Si_3H_8 in sc-hexane at 420 °C and 34.5 MPa (5000 psi) for 10 min. The particles are spherical and relatively monodisperse. The average diameter of the particles depended on the amount of Si_3H_8 used in the reaction, ranging from as small as 170 nm up to about 1.7 μm , increasing in diameter as the Si_3H_8 is increased. The standard deviation about the mean diameter is less than 10% in some cases (Figure 1A for example). The smallest particles obtained using this method are about 170 nm in diameter, as reactions carried out with less Si_3H_8 give very little product.

XRD showed that the particles are composed of hydrogenated amorphous silicon (a-Si:H). Figure 2 shows

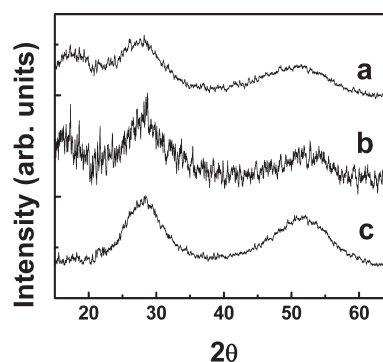


Figure 2. XRD of a-Si:H particles synthesized in sc-hexane at 34.5 MPa (5000 psi), 20 μL trisilane, and (a) 380, (b) 425, and (c) 500 °C. The broad diffraction peaks at 2θ values of 52° and 28.5° are characteristic of a-Si:H.^{23,29–32}

XRD patterns of three different samples made at varying reaction temperatures of 380, 425, and 500 °C. The diffraction data exhibit two broad diffraction peaks at 2θ values of 28.5° and 52°, characteristic of amorphous Si.^{23,29–32}

The particle morphology and optical properties were strongly affected by the reaction temperature. As shown in Figure 3, the color of the colloidal product varied from bright yellow, for the particles synthesized at the lowest temperature of 380 °C, to red to a very dark purple (almost black) as the reaction temperature was increased to 550 °C. As discussed below in detail, the difference in color is due to the difference in hydrogen content and extent of bond order of the a-Si:H in the particles that was found to depend strongly on the reaction temperature. The reaction temperature also affected the amount of aggregation between particles. Reaction temperatures greater than about 450 °C led to significant aggregation with necking and some sintering between neighboring particles. Reaction temperatures below 400 °C gave non-aggregated particles, but with rougher surfaces and a broader size distribution than those made at slightly higher temperature. Reactions carried out between 400 and 420 °C produced particles with smooth surfaces, and the most monodisperse size distributions without aggregation. The reaction pressure also affected the quality of the product. Pressures below 24 MPa produced large aggregates of a-Si with no spherical particles. Reactions carried out at pressures in the range of 27–45 MPa exhibited similar quality, like those shown in Figures 1 and 3. Reactions at pressures greater than 45 MPa were not tested due to the safety limitations of the reactor system.

Si–Si Bond Order in the a-Si:H Particles. The wide range of colors exhibited by particles made at different temperature indicates that there are significant differences in structural order and hydrogen content between the samples, as the optical gap of a-Si is known to vary widely, from 1.55 to 2.1 eV, with increasing structural

- (26) Viera, G.; Huet, S.; Boufendi, L. *J. Appl. Phys.* **2001**, *90*, 4175–4183.
 (27) Gajovic, A.; Gracin, D.; Juraic, K.; Sancho-Parramon, J.; Ceh, M. *Thin Solid Films* **2009**, *517*, 5453–5458.
 (28) Tsu, D. V.; Chao, B. S.; Jones, S. J. *Sol. Energ. Mat. Sol. C* **2003**, *78*, 115–141.

- (29) Mahan, A. H.; Yang, J.; Guha, S.; Williamson, D. L. *Phys. Rev. B* **2000**, *61*, 1677–1680.
 (30) Mamiya, M.; Takei, H.; Kikuchi, M.; Uyeda, C. *J. Cryst. Growth* **2001**, *229*, 457–461.
 (31) Williamson, D. L. *Sol. Energ. Mat. Sol. C* **2003**, *78*, 41–84.
 (32) Guha, S.; Yang, J.; Williamson, D. L.; Lubianiker, Y.; Cohen, J. D.; Mahan, A. H. *Appl. Phys. Lett.* **1999**, *74*, 1860–1862.

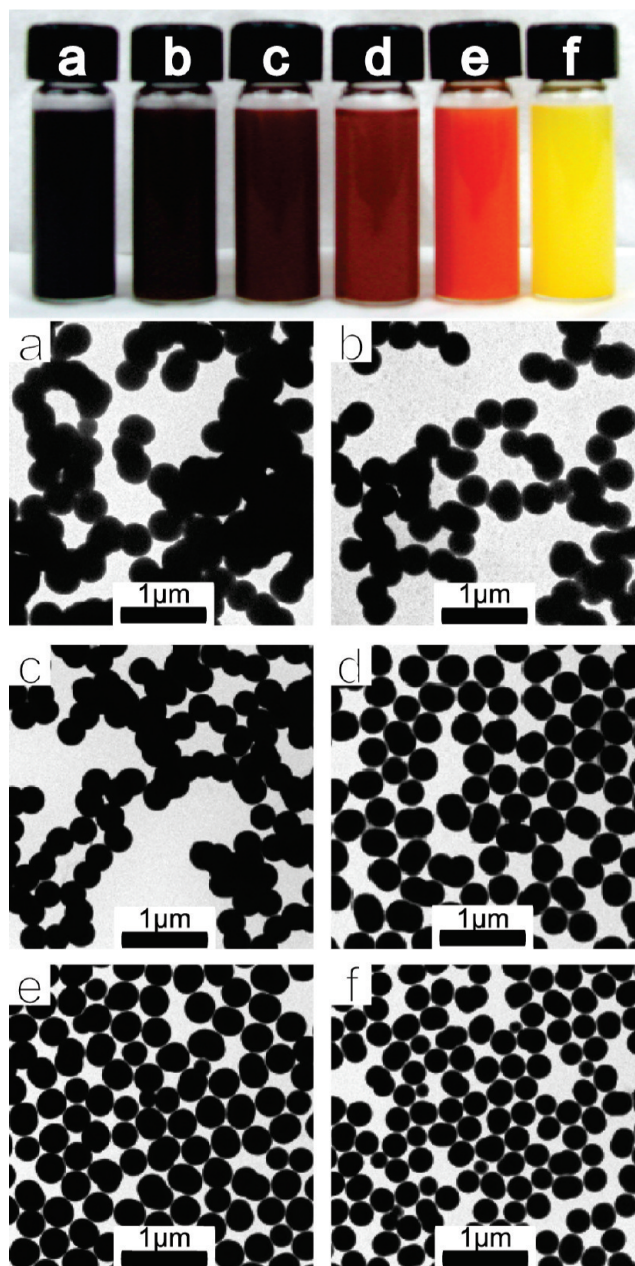


Figure 3. (Top) Photograph of vials of a-Si:H particles dispersed in chloroform that were made at temperatures of (a) 550, (b) 500, (c) 450, (d) 420, (e) 400, and (f) 380 °C. (Bottom) TEM images of the particles from the dispersions shown in the top panel. The labels correspond to those in the photograph. Particles were synthesized with 5 μL of Si_3H_8 in sc-hexane at 34.5 MPa (5000 psi).

order and hydrogen content.^{33–35} XRD (Figure 2) did not reveal any evidence that varying reaction temperature led to changes in the structural order within the a-Si:H particles, as there was no observable shift in diffraction peak position or peak widths. XRD, however, can only detect microcrystallinities as low as 10%.³² Raman spectroscopy is a much more sensitive probe than XRD to local atomic arrangements. Figure 4 shows Raman spectra

of a-Si:H particles synthesized at different temperatures and Si_3H_8 concentrations. The broad Raman band at $\sim 475\text{ cm}^{-1}$ characterizes amorphous Si. It is associated with the a-Si transverse optical (TO) mode and the stretching vibrations of the Si–Si bonds in the silicon tetrahedron.^{26,28} When probed at 10% laser power, all of the particle samples exhibited this Raman band. As the synthesis temperature was increased, the particles exhibited a second Raman signal at $\sim 490\text{--}496\text{ cm}^{-1}$, indicating a higher amount of bond order in those samples. This trend became more evident when larger initial concentrations of Si_3H_8 were used in the reactions (Figure 4a–c).

The particles synthesized at higher temperature could be crystallized under the probe laser used for the Raman experiments. When Raman spectra were obtained for particles made at 420 and 450 °C using illumination at 50% or higher power incidences (1.5–5.0 mW), a sharp Raman peak centered at $516\text{--}518\text{ cm}^{-1}$ was observed. When the particles made at 420 and 450 °C were again probed with the laser attenuated to only 10% power (0.35 mW), they still showed a sharp Raman peak centered at $516\text{--}518\text{ cm}^{-1}$. This peak arises from microcrystalline Si ($\mu\text{c-Si}$),^{26,36,37} and indicates that the a-Si:H particles were crystallized by laser irradiation. Conversely, the particles synthesized at 380 °C did not crystallize under the Raman probe laser, even when operated at full laser power. The fact that the particles made at 380 °C did not crystallize under the laser indicates that these particles were much more amorphous in character than those made at higher temperature. The observed differences in crystallization dynamics were also found to correlate with the relative intensity of the Raman contribution at $490\text{--}496\text{ cm}^{-1}$ (Figure 4g). According to a model of phonon confinement, this peak can be assigned to the presence of 1–2 nm domains of ordered Si.^{26,38} Note that the most extensively used correlation length confinement model is not valid for such small diameters (minimum 4 nm).^{26,36,37} The presence of Si clusters in the amorphous Si matrix would seed crystallization, and likewise the absence of those seeds (as in the particles prepared at 380 °C (Figure 4g)) would lead to the observed slow crystallization dynamics.²⁶ Analysis of the Raman spectra showed that there was an increase in the volume fraction of the bond-ordered Si clusters in the particles synthesized at higher reaction temperature (Figure 4h). There was also a slight increase in the volume fraction of these clusters with increased initial Si_3H_8 concentrations (Figure 4h). Although it is possible that laser heating, even at only 10% power incidence, could increase the apparent amount of ordered Si clusters in the particles, it is clear that the particles synthesized at higher temperatures possess a higher degree of structural order within the a-Si:H matrix, either in the form of 1–2 nm diameter clusters of bond-ordered Si²⁶

- (33) Cody, G. D.; Tiedje, T.; Abeles, B.; Brooks, B.; Goldstein, Y. *Phys. Rev. Lett.* **1981**, *47*, 1480–1483.
 (34) Sokolov, A. P.; Shebanin, A. P.; Golikova, O. A.; Mezdrogina, M. M. *J. Phys.-Condens. Matter* **1991**, *3*, 9887–9894.
 (35) Fukutani, K.; Kanbe, M.; Futako, W.; Kaplan, B.; Kamiya, T.; Fortmann, C. M.; Shimizu, I. *J. Non-Cryst. Solids* **1998**, *227*, 63–67.

- (36) Richter, H.; Wang, Z. P.; Ley, L. *Solid State Commun.* **1981**, *39*, 625–629.
 (37) Campbell, I. H.; Fauchet, P. M. *Solid State Commun.* **1986**, *58*, 739–741.
 (38) Zi, J.; Buscher, H.; Falter, C.; Ludwig, W.; Zhang, K. M.; Xie, X. D. *Appl. Phys. Lett.* **1996**, *69*, 200–202.

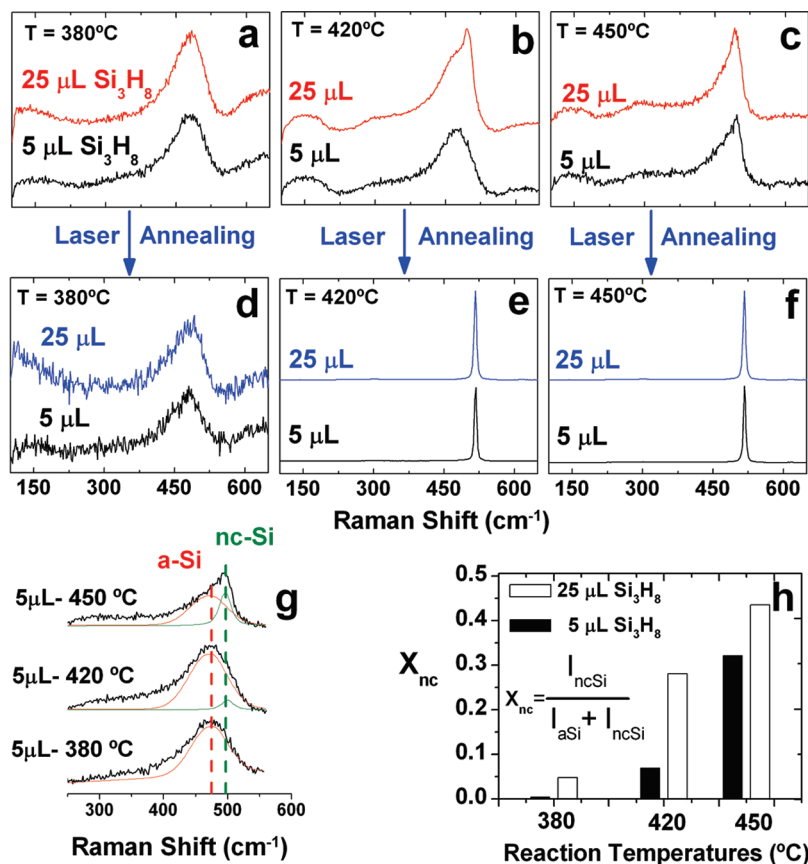


Figure 4. Raman spectra ($\lambda_{exc} = 514.5$ nm) of a-Si:H particles made at different reaction temperature and Si₃H₈ concentration. Graphs a–c show the spectra obtained with the laser attenuated to 10% (0.35 mW) of its maximum power for the particles synthesized at (a) 380, (b) 420, and (c) 450 °C. Graphs d–f correspond to those same particles after exposure at 50% (1.5 mW) laser power, collected with laser again attenuated to 10% power. Within each graph, the upper and lower curves correspond to particles synthesized with 25 and 5 μ L of Si₃H₈, respectively. Graph g shows the fitting of amorphous and crystalline contributions of the samples prepared with 5 μ L of Si₃H₈ and exposed to 10% laser power. Fittings were obtained by utilizing Gaussian (a-Si:H) or a combination of Lorentzian–Gaussian (nc-Si) curves. Graph h shows the estimated volume fraction (X_{nc}) of 1–2 nm nanocrystallites embedded in the a-Si:H matrix. X_{nc} was obtained from the ratios of fitted integrated areas associated with the 1–2 nm nanocrystalline (490–495 cm⁻¹) and amorphous (475–480 cm⁻¹) phases corresponding to spectra a–c. All samples were synthesized in 34.5 MPa (5000 psi) sc-hexane with 10 min of heating.

or as randomly distributed networks with intermediate bond order as described by Tsu et al.,²⁸ which enhance the rate of crystallization upon laser annealing.

H-Content in the a-Si:H Particles. It is well-known that structural order tends to be correlated with hydrogen content in a-Si:H.^{33,34} Indeed, ATR-FTIR spectroscopy and TGA/DSC revealed significant differences in hydrogen content between the samples. In ATR-FTIR spectroscopy, hydrogenated Si species tend to appear as spectral features related to Si–H, Si–H₂, and (Si–H₂)_x chains.^{39,40} TGA/DSC provides a quantifiable signature of hydrogen evolution when the sample is heated.

Figure 5 shows ATR-FTIR spectra of a-Si:H particles synthesized at a range of temperature. Peaks at ~ 2100 and 900 cm⁻¹, corresponding to a Si–H stretches, were present in all of the spectra.⁴¹ The spectra in Figure 5 have been normalized to the Si–H stretching frequency peak at ~ 2100 cm⁻¹. The presence of the peak at 870 cm⁻¹

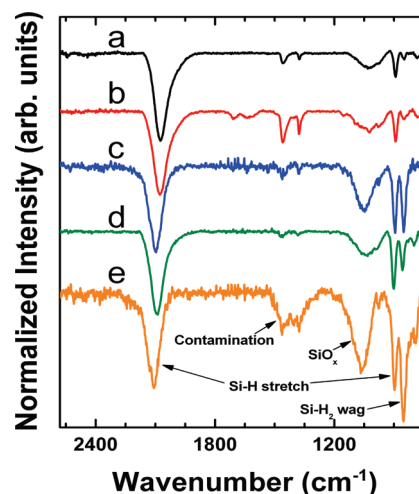


Figure 5. ATR-FTIR spectra of a-Si:H particles synthesized in sc-hexane at 34.5 MPa (5000 psi) with 25 μ L of Si₃H₈ at various temperatures of (a) 450, (b) 425, (c) 420, (d) 400, and (e) 380 °C. The spectra have been normalized to the intensity of the Si–H stretch at 2100 cm⁻¹.

corresponding to the Si–H₂ wag, also provides an indication of how extensively hydrogenated the samples were. Particles made at 380 °C had a significantly more intense peak at 870 cm⁻¹ than at 900 cm⁻¹, indicating a large

- (39) Webb, J. D.; Gedvilas, L. M.; Crandall, R. S.; Iwaniczko, E.; Nelson, B. P.; Mahan, A. H.; Reedy, R.; Matson, R. J. *Mater. Res. Soc. Symp. Proc.* **1999**, 557, 311–316.
 (40) Roura, P.; Farjas, J.; Rath, C.; Serra-Mirallès, J.; Bertran, E.; Cabarrocas, P. R. I. *Phys. Rev. B* **2006**, 73, 085203.
 (41) Lucovsky, G.; Nemanich, R. J.; Knights, J. C. *Phys. Rev. B* **1979**, 19, 2064–2073.

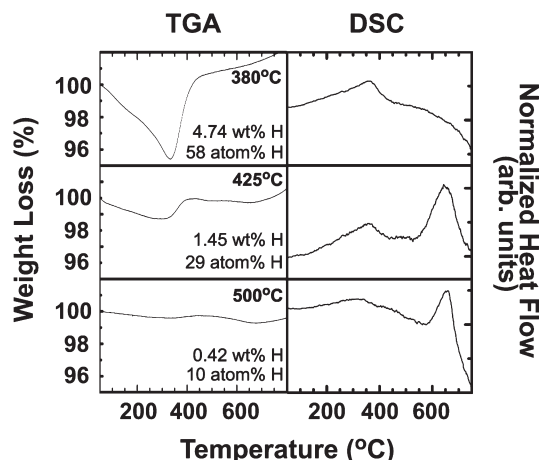


Figure 6. TGA/DSC data for a-Si:H particles synthesized with 50 μL Si_3H_8 in sc-hexane at 34.5 MPa (5000 psi) and temperatures of 380, 425, or 500 $^{\circ}\text{C}$. The temperature was increased at a rate of 5 $^{\circ}\text{C}/\text{min}$ under flowing nitrogen. The weight loss in the sample is attributed to hydrogen desorption.

amount of hydrogen loading in those particles. The peak at 870 cm^{-1} was lower in intensity relative to the peak at 900 cm^{-1} for particles made at higher temperatures, indicating less Si hydrogenation. When the reaction temperature was increased from 420 to 425 $^{\circ}\text{C}$, there was a particularly noticeable difference in the spectra. Particles made at 420 $^{\circ}\text{C}$ had a fairly significant Si–H₂ wag at 870 cm^{-1} , whereas particles made at 425 $^{\circ}\text{C}$ did not exhibit this peak. There appears to be a qualitative change in the decomposition pathway of trisilane and Si incorporation into the growing particles at this temperature. ATR-FTIR spectra of particles made at 450 $^{\circ}\text{C}$ do not exhibit the Si–H₂-related peak.

The ATR-FTIR spectra clearly show that the hydrogen content is significantly higher in particles synthesized at lower temperature. TGA/DSC provided a quantitative estimate of the hydrogen loading in the samples. As shown in Figure 6, there is significant weight loss when the samples were heated. The majority of this weight loss is the result of hydrogen desorption. The hydrogen content in the a-Si:H particles was significantly higher when lower synthesis temperatures were used, increasing from 10 to 29 to 58 atomic % when the synthesis temperature was changed from 500 to 425 and to 380 $^{\circ}\text{C}$, respectively. After hydrogen evolved from the sample, there was then a significant weight gain due to oxidation by residual oxygen in the chamber and the nitrogen source. The weight gain due to oxidation was largest for the particles made at the lowest temperature of 380 $^{\circ}\text{C}$. The weight gain due to oxidation also obscures the weight loss due to hydrogen desorption, so the reported hydrogen contents represent lower bound estimates. Unsatisfied Si bonds

left by desorbed hydrogen appear to be more easily attacked by oxygen in these samples. There is also a small exothermic peak in the DSC scan at ~ 340 $^{\circ}\text{C}$, when most of the hydrogen has desorbed and the particles are rapidly oxidizing.¹³ The particles synthesized at 425 and 500 $^{\circ}\text{C}$ exhibited exothermic spikes at 650 $^{\circ}\text{C}$ due to the crystallization of the a-Si core.^{7,42} Particles made at 380 $^{\circ}\text{C}$ did not exhibit this feature in the DSC data, indicating that there was no crystallization, most likely due to a prohibitively large amount of structural disorder in the particles and the absence of any nanocrystalline clusters.

Summary

Colloidal a-Si:H particles can be produced by Si_3H_8 decomposition in sc-hexane with a fairly wide range of size, hydrogen content and structural order, depending on the synthesis temperature, pressure and reactant concentration. Higher temperature reactions produced particles with more structural order and less associated hydrogen. Particles made at 450 $^{\circ}\text{C}$ or higher were also slightly agglomerated. Raman spectroscopy was used as a sensitive probe to examine structural differences in the particles made at different temperature. The excitation laser used for Raman spectroscopy had enough power to crystallize particles that were synthesized at temperatures higher than 380 $^{\circ}\text{C}$ because of the presence of regions with intermediate bond order or 1–2 nm diameter bond-ordered Si clusters that serve to nucleate crystallization. As far as we are aware, the reported method is the only available solution-phase approach to a-Si:H particles. Future work now involves examining their properties, including electrochemical studies on the potential of a-Si:H particles as a recipient for Li⁺ implantation and the effects of hydrogen content on this process. The high hydrogen contents will also be tested for ease of removal and potential cyclability.

Acknowledgment. This material is based upon work supported as part of the program “Understanding Charge Separation and Transfer at Interfaces in Energy Materials and Devices (EFRC:CST),” an Energy Frontier Research Center funded by the U.S. Department of Energy, Office of Science, Office of Basic Energy Sciences under Award Number DE-SC0001091. J.L.H. acknowledges support from a Fundación Alfonso Martín Escudero Postdoctoral Fellowship. Funding for the Rigaku Spider X-ray diffractometer from the National Science Foundation Grant No. 0741973 is also acknowledged. We thank Dr. Andrew Heitsch for many insightful discussions about trisilane chemistry and particle growth in high-temperature supercritical solvents.

(42) Spinella, C.; Lombardo, S.; Priolo, F. *J. Appl. Phys.* **1998**, *84*, 5383–5414.